Sulfur Impregnation on Activated Carbon Fibers through H_2S Oxidation for Vapor Phase Mercury Removal

Wenguo Feng[1]; Seokjoon Kwon[2]; Xue Feng[3]; Eric Borguet[4]; and Radisav D. Vidic, M.ASCE[5]

Abstract: Sulfur was impregnated onto activated carbon fibers (ACFs) through H_2S oxidation catalyzed by the sorbent surface in a fixed-bed reactor. By changing the temperature and duration of the sulfur impregnation process, ACFs with different sulfur contents were developed. Characterization of ACFs before and after sulfur impregnation was conducted by surface area analysis, energy dispersive X-ray analysis, thermogravimetric analysis, X-ray photoelectron spectroscopy, and temperature programmed desorption. Vapor phase mercury adsorption experiments were carried out in a fixed-bed reactor. Sulfur was impregnated mainly as elemental sulfur and the amount of sulfur deposited on the ACF increased with an increase in impregnation temperature. Higher temperature leads to more uniform sulfur distribution inside the sorbent pores. The impregnation process can be explained by a combination of pore filling and monolayer adsorption, with the former mechanism predominating at low temperatures. In the absence of sulfur, the mercury adsorption capacity can be correlated with surface area and pore volume.

DOI: 10.1061/(ASCE)0733-9372(2006)132:3(292)

CE Database subject headings: Activated carbon; Sulfur; Mercury; Hydrogen sulfides; Oxidation; Abatement and removal.

Introduction

Mercury is a toxic air pollutant that has attracted significant public health and environmental attention recently. Its emission from anthropogenic sources comprises a significant portion of the total mercury released to the environment. It was estimated that approximately 150 tons of mercury is emitted annually by power plants, municipal waste incinerators, and other industrial sources in the United States (EPA 1997). Mercury is emitted in two major forms: elemental and oxidized mercury (Hg^+ or Hg^{2+} combined with other elements such as Cl and O). Control of elemental mercury emissions is more difficult due to its high volatility and low solubility.

[1]PhD Candidate, Dept. of Civil and Environmental Engineering, Univ. of Pittsburgh, 975 Benedum Hall, Pittsburgh, PA 15261. E-mail: wef3@pitt.edu

[2]Postdoctoral Scientist, Connecticut Agricultural Experimental Station, 123 Huntington St., P. O. Box 1106, New Haven, CT 06504. E-mail: Joon.kwon@po.state.ct.us

[3]PhD Candidate, Dept. of Civil and Environmental Engineering, Univ. of Pittsburgh, 968 Benedum Hall, Pittsburgh, PA 15261. E-mail: fengxue_2002@yahoo.com

[4]Associate Professor, Dept. of Chemistry, Temple Univ., 1901 N. 13th St., Philadelphia, PA 19122. E-mail: eborguet@temple.edu

[5]Professor, Dept. of Civil and Environmental Engineering, Univ. of Pittsburgh, 943 Benedum Hall, Pittsburgh, PA 15261 (corresponding author). E-mail: vidic@pitt.edu

Note. Discussion open until August 1, 2006. Separate discussions must be submitted for individual papers. To extend the closing date by one month, a written request must be filed with the ASCE Managing Editor. The manuscript for this paper was submitted for review and possible publication on June 17, 2004; approved on July 19, 2005. This paper is part of the ***Journal of Environmental Engineering***, Vol. 132, No. 3, March 1, 2006. ©ASCE, ISSN 0733-9372/2006/3-292–300/$25.00.

Adsorption by high surface area activated carbon is among the most promising technologies for mercury removal. While raw activated carbon can be effective in removing mercury at high sorbent to mercury ratios (Chang and Offen 1995; EPA 1997; Flora et al. 2003), impregnation of functional groups, especially sulfur, can significantly improve the adsorption capacity.

A previous study (Sinha and Walker 1972) tested mercury adsorption capacity of sulfur impregnated activated carbon that was produced through H_2S oxidation at 140°C. The time for breakthrough of mercury from a fixed-bed adsorber at room temperature decreased with an increase in sulfur content. Such behavior was explained by the narrowing of micropores in the virgin sorbent through sulfur deposition. However, at 150°C, the sulfurized carbon had much higher capacity than the original carbon. Otani et al. (1988) added sulfur onto an activated carbon surface by soaking in CS_2 solution. Mercury adsorption capacity was found to increase with an increase in sulfur content up to 13% and no decrease in mercury adsorption capacity was observed even for very high sulfur content on the sorbent. The writers suggested that a decrease in activated carbon surface area in their method of sulfur impregantion was less pronounced than that in the method used before (Sinha and Walker 1972).

Impregnation of sulfur onto activated carbon through the reaction between elemental sulfur and the carbon surface at elevated temperatures was studied by Vidic and co-workers (Korpiel and Vidic 1997; Liu et al. 1998; Kwon and Vidic 2000). Their studies suggested that the following factors are important for mercury uptake by sulfur impregnated sorbents: sulfur content, sulfur forms, sulfur distribution, and pore structure/surface area of the sorbent. Sulfur impregnated carbons produced at higher impregnation temperatures (400–600°C) performed better than those produced at lower temperatures (25–150°C). The writers suggested that higher temperature produced shorter chain sulfur allotropes and more uniform sulfur distribution on the sorbent's surface. Liu et al. (1998) tested the impact of temperature and the

initial sulfur to carbon mass ratio on developing a better sorbent for mercury removal. The impregnation temperature was found to be more important than the sulfur to carbon mass ratio. This was attributed to the fact that sorbents generated under higher temperature still retained their high surface area and mesoporous structure. Kwon and Vidic (2000) compared mercury adsorption capacity of BPL carbon impregnated with S through two different methods: reaction with elemental sulfur at 600°C and oxidation of H_2S at 150°C. They found the former method to be much more effective in producing high capacity sorbents than the latter. Sorbents impregnated through H_2S oxidation exihibited highly nonlinear correlation between sulfur content and mercury uptake capacity, with optimal sulfur content around 5% by weight (Kwon and Vidic 2000). Sulfur impregnation through H_2S oxidation has significant value in the industrial ecology approach for producing effective sorbents (the waste stream from one process serves as a raw material for another process).

Sulfur impregnation of activated carbon fibers (ACFs) was studied by Hsi et al. (2001, 2002). ACFs have uniform pore structures with most of the pores in the micropore region ($d<2$ nm). ACF impregnated with elemental sulfur at 400°C was found to be the most effective mercury sorbent (Hsi et al. 2001). Although this sorbent had a surface area of only 94 m^2/g, 86% of the surface area was attributed to micropores. Sulfur deposited on ACF existed in three forms, namely, elemental sulfur, organic sulfur, and sulfate, with only the first two forms acting as mercury adsorption sites (Hsi et al. 2002). The writers suggested that both sulfur content and micropore structure are important for the uptake of vapor phase mercury.

Daza et al. (1989) applied various techniques to characterize palygorskite [a fibrous mineral with hydrated magnesium silicate $Mg_3Si_4O_{10}(OH)_2$] impregnated with sulfur through catalytic oxidation of hydrogen sulfide. The impregnation was achieved in a fixed-bed reactor operated at 140°C with $O_2:H_2S=1:1$. They found that the π form of sulfur and a pore diameter larger than about 7.5 nm yielded the best sorbents. In addition, the writers proposed that monolayer coverage of sulfur molecules on the internal surface will produce the most efficient sorbent for Hg removal. They also suggested that pore structure that creates no steric hindrance for HgS formation is a general requirement for good mercury sorbent with a minimum pore size per monolayer of deposited sulfur of around 8 nm (Daza et al. 1993). Guijarro et al. (1998) tested mercury uptake capacity of sulfurized sepiolite and suggested that macropores above 400 nm are the most important for mercury uptake because high surface area sorbents with small pores impregnated with high sulfur content would result in quick blockage of the pore entrance by HgS.

Oxidation of H_2S at room temperature on activated carbon was studied by Bandosz and co-workers (Bagreev et al. 1999; Bandosz 1999; Bagreev and Bandosz 2001; Bagreev et al. 2001; Bagreev and Bandosz 2002; Bandosz 2002). They suggested that products of H_2S oxidation were mainly elemental sulfur and sulfuric acid (Bandosz 1999; 2002). They also found that basic conditions favor the formation of elemental sulfur (Bandosz 2002). Yan et al. (2002, 2004) suggested that elemental sulfur and oxidized sulfur species were major products of H_2S oxidation on activated carbon surface at low temperature and in the presence of water vapor.

However, further work focusing on oxidation of hydrogen sulfide on carbonaceous surfaces is still needed to better understand the mechanism behind mercury sorbent development. The objective of this study was to determine the process of sulfur impregnation on carbonaceous surfaces through H_2S oxidation and to determine sulfur forms that are created through this process. An additional objective was to understand the key parameters of sulfur impregnated sorbents for elemental mercury adsorption in light of the findings available in the literature.

Experimental Details

Activated Carbon Fibers

The carbonaceous sorbent selected for this study was activated carbon fiber, which has fairly uniform pore size distribution. ACFs obtained from American Kynol, Inc. have carbon content of over 95% and were produced from the novolac resin that is manufactured by polymerization of phenol and formaldehyde. With the increase in serial numbers (ACF10, ACF20, and ACF25), the total surface area and pore volume were expected to increase due to prolonged activation time. The serial number is designated by the manufacturer to represent the expected surface area per gram of ACF. For example, ACF10 has a surface area of around 1,000 m^2/g while ACF25 has a surface area of around 2,500 m^2/g The most important characteristic regarding the pore size distribution is that the slit shaped micropores below 2 nm in width are predominant, with very few pores in the mesopore range ($2<d<50$ nm) and no pores in the macropore range (>50 nm). ACFs were dried at 120°C for 2 h and ground into powder before sulfur impregnation.

Sulfur Impregnation by H_2S Oxidation

Fig. 1 shows the experimental setup for sulfur impregnation by H_2S oxidation. The gases were supplied from pressurized tanks. H_2S (Praxair, 5% in nitrogen, certified) and O_2 (Praxair, pure) were diluted by N_2 (Praxair, ultrahigh purity) to a desired concentration by controlling the flow rate of each gas with a mass flow controller. The molar ratio of O_2 to H_2S in the incoming gas was always maintained at 4 to 1. The total gas flow rate to a quartz reactor (38 cm long with 1 cm outside diameter) was maintained at 150 mL/min. The reactor was positioned vertically in the middle of a tubular furnace (Lindberg Heavi-Duty, Watertown, Wis.). The effluent gases were analyzed continuously by a quadrupole mass spectrometer (QMS 300, Stanford Research Systems, Sunnyvale, Calif.).

ACF10 was impregnated with sulfur at 80 and 150°C until the effluent H_2S concentration reached the influent level after 16 to 24 h. These samples were labeled as ACF10-80C and ACF10-150C. ACF25 was impregnated with sulfur at 150°C for 2, 6, and 24 h. Designation for these sorbents includes temperature and duration of the impregnation process, i.e., ACF25-150C-2 h means the ACF25 was impregnated with H_2S at 150°C for 2 h. As received ACFs were designated as "ACF10-raw" and "ACF25-raw."

The amount of sulfur deposited on the sorbent was determined from the breakthrough curve assuming that all H_2S eliminated from the stream was deposited onto the ACF surface.

Sorbent Characterization

The surface area and pore size distribution of virgin and impregnated ACFs were analyzed using nitrogen adsorption at 77 K in a Quantachrome Autosorb Automated Gas Sorption System (Quantachrome Corporation, Boynton Beach, Fla.).

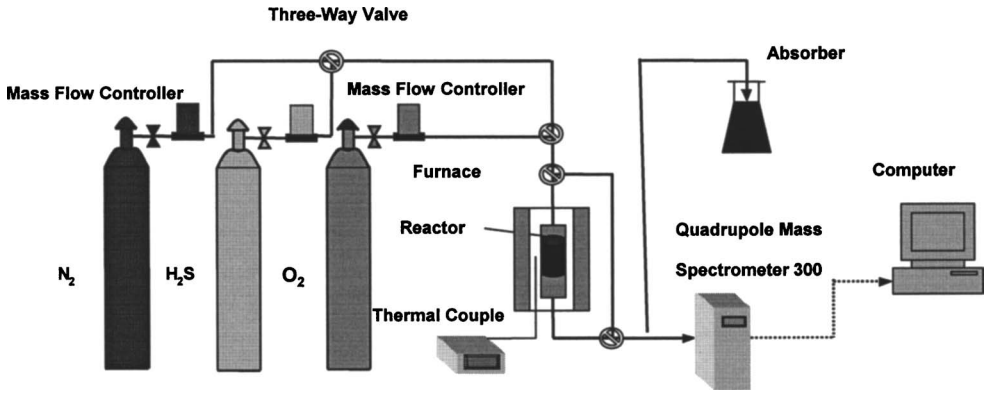

Fig. 1. Experimental setup for sulfur impregnation by H_2S oxidation

Thermogravimetric analysis (TGA) was conducted using TGA7 (Perkin-Elmer, Norwalk, Conn.) where the sample was maintained at 120°C for 2 h and then heated to 800°C with a heating rate of 10°C/min in a high purity nitrogen atmosphere.

The TGA data can also be used to estimate the activation energy for the desorption of impregnated sulfur from the carbon surface. TGA analysis of a sample (ACF10-150C-24 h) at different heating rates (2, 6, 10, and 14°C/min) yields different rates of weight loss versus temperature. The activation energy can be estimated according to the following equation (Flynn and Wall 1966)

$$E_a = -18.18 d(\log B)/d(1/T)$$

where E_a=activation energy for desorption in J/mol; B=heating rate in K/s; and T=temperature corresponding to a given weight loss at a given heating rate in K.

Temperature programmed desorption (TPD) was conducted using TGA that was coupled to the QMS 300 to sample the effluent gas from the TGA. This method enabled simultaneous detection of the weight loss and gas species released from ACF10-raw and ACF10-150C. However, elemental sulfur released during heating was observed to quickly condense as yellow solid at the outlet of the TGA chamber, and could not be detected by the QMS. The heating rate in the TPD experiment was 60°C/min with a nitrogen flow rate of 12 mL/min.

Scanning electron microscope (SEM)–energy dispersive X-ray analysis (EDAX) analysis was conducted using a Philips XL30 SEM equipped with an EDAX detector. Besides observing the image of ACFs, the EDAX detector was used to measure the elemental composition of the ACF samples that were pasted as a thick layer onto a tape before insertion into the vacuum chamber.

X-ray photoelectron spectroscopy (XPS) analysis was performed using a Physical Electronics Model 550 equipped with a cylindrical, double-pass energy analyzer. The ACF samples were attached to a tantalum surface by a conductive silver paste (LADD Research Industries) before insertion into the vacuum chamber.

Mercury Adsorption Test

Raw (or virgin) and sulfur-impregnated ACFs were tested for vapor phase elemental mercury uptake at 140°C in a fixed-bed reactor system (Kwon and Vidic 2000). This system is composed of a gas supply unit, a mercury permeation tube, a quartz tube reactor, a furnace, and a mercury detection unit.

Industrial grade nitrogen (99.5%) was used as the carrier gas with a flow rate of 600 mL/min, which is controlled by a mass flow controller (Tylan General, Torrance, Calif.). The inlet mercury concentration was maintained at 350 $\mu g/m^3$ by controlling the temperature of the permeation tube filled with liquid mercury (VICI Metrons Inc., Santa Clara, Calif.).

Mercury concentration was analyzed continuously using an atomic absorption spectrophotometer (Model 403, Perkin-Elmer, Norwalk, Conn.) equipped with an 18 cm hollow quartz cell (Varian Australis Pty, Ltd., Mulgrave, Victoria, Australia) and the mercury adsorption capacity was calculated by integrating the area above the breakthrough curve.

Although ACF-20-raw was not used for the sulfur impregnation experiments, it was included into the mercury uptake test to investigate the effect of pore structure on mercury uptake.

Results and Discussion

Structure of Raw ACFs

Fig. 2 depicts pore size distribution of raw ACFs after grinding into powders. It is clear that the diameter of most pores in these ACFs is below 2 nm. These micropores can be divided into three ranges corresponding to three peaks on Fig. 2: small ($d<0.72$ nm), medium ($0.72<d<0.90$ nm), and big micropores ($d>0.90$ nm). As the serial number increases from ACF10 to ACF25, medium and big micropore volume (>0.72 nm) increases while the small micropore volume (<0.72 nm) decreases. This is not surprising because ACFs with increasing serial numbers were produced under extended activation time.

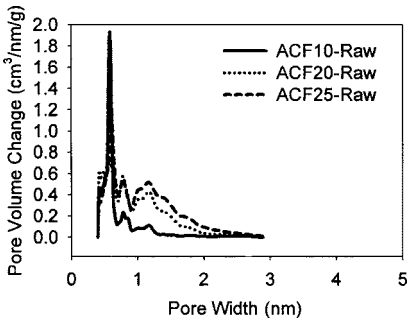

Fig. 2. Pore size distribution of raw ACFs

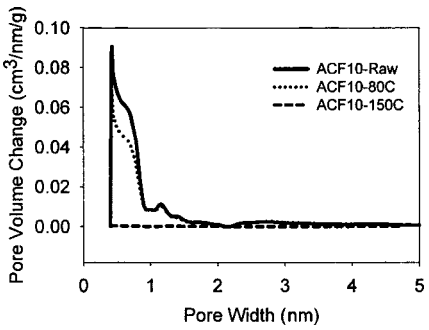

Fig. 3. Pore size distribution of ACF-10 before and after sulfur impregnation

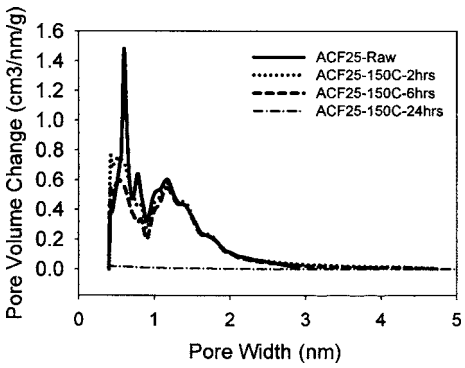

Fig. 4. Pore size distribution of ACF-25 before and after sulfur impregnation

Sulfur Content and Distribution

Table 1 summarizes general properties of the sorbents produced in this study and their respective Hg uptake capacities. It is clear from these results that low temperature (e.g., 80°C) does not facilitate significant sulfur deposition through H_2S oxidation, even if a complete H_2S breakthrough was attained. Both ACF10 and ACF25 achieved much higher sulfur content at 150°C. This is due to the fact that a predominant mechanism for H_2S adsorption at low temperatures is physisorption (Boki and Tanada 1980; Aranovich and Donohue 1995; Lee and Reucroft 1999), which leads to filling of small micropores ($d<0.72$ nm) first. As a result, the catalytic oxidation of H_2S could only take place in small micropores. This hypothesis is supported by pore size distribution measurements shown in Fig. 3, which depicts changes in the pore size distribution of ACF10 after sulfur impregnation at 80 and 150°C. It is clear that sulfur deposition at 80°C is accomplished more by pore filling than by monolayer deposition as the loss in the small micropores is obvious, while very few medium micropores were occupied by sulfur molecules.

Fig. 4 shows changes in the pore size distribution of ACF25 as a result of sulfur impregnation at 150°C for 2, 6, and 24 h. It is clear that the initial losses in the pore volume after only 2 h of impregnation occurred in small and medium micropores, while large micropores were not affected by sulfur deposition. The loss of small micropores was also observed by Hsi et al. (2001, 2002). As the impregnation time was extended to 6 h, further reduction in small and medium size micropores was observed. Reduction in the large micropore volume was observed only after the amount of sulfur deposited on the ACF surface exceeded 20 wt % after 24 h of impregnation. A similar conclusion can be made for the data shown in Fig. 3 and Table 1, where the sulfur content exceeded 20% by weight before filling of large micropores was accomplished.

SEM-EDAX analysis was conducted for ACFs before and after sulfur impregnation. EDAX provided the elemental composition (% wt) of the outer layer of the ACF samples. The results obtained at 15 kV are shown in Table 2. Sulfur content based on QMS detection, which represent the average sulfur content (% wt) of the sample, is also listed in the same table. At low temperatures (i.e., 80°C) and short impregnation times (i.e., 2 and 6 h), sulfur content at the outer surface of the ACF is much lower than the bulk average. This means that sulfur tends to deposit more inside the fibers than on the outside at lower impregnation temperatures and during the initial stages of impregnation at higher temperatures. However, pore filling is not the only mechanism for sulfur deposition on ACF. Some sites at the outer surface, especially at high temperatures, were also important for sulfur deposition because the sulfur content on the outer surface was higher than the bulk average after 24 h of impregnation, when almost all pores are filled or blocked. In addition, sulfur is melted at a temperature of 150°C, which may also achieve a more uniform distribution of sulfur on the carbon surface.

It is clear that pore size analysis conducted through nitrogen adsorption measurements cannot determine if the loss in pore volume is due to sulfur deposition by complete filling of the pores or just blockage of the pore entrance. This question can only be answered by calculating the volume of sulfur added per gram of ACF and comparing it with the lost pore volume. The volume of

Table 1. Summary of Sorbent Properties and Mercury Adsorption Capacity

Sample name	S content (% wt)	V_s (cm^3/g)	V_m (cm^3/g)	V_b (cm^3/g)	V_t (cm^3/g)	BET surface area[a] (m^2/g)	Hg uptake capacity ($\mu g/g$)	S utilization ratio (%)
ACF10-raw	0.2	0.274	0.039	0.065	0.371	920	214	—
ACF10-80 C	6.7	0.164	0.040	0.095	0.299	710	450	0.107
ACF10-150 C	26.3	0.001	0.001	0.003	0.005	8	220	0.013
ACF25-raw	0.2	0.263	0.101	0.489	0.741	1,950	319[b]	—
ACF25-150 C-2 h	4.1	0.227	0.069	0.454	0.714	1,880	790	0.307
ACF25-150 C-6 h	10.2	0.173	0.052	0.409	0.634	1,610	480	0.075
ACF25-150 C-24 h	30.5	0.006	0.002	0.007	0.015	100	230	0.012

Note: V_s=small micropore volume; V_b=big micropore volume; V_m=medium micropore volume; and V_t=total pore volume.

[a]Pressure used: $P/P_0=1.0\times10^{-5}\sim1.0$.

[b]Deviation was ±8% based on three runs.

Table 2. Comparison of Surface (EDAX Results) and Average Sulfur Content (QMS Results)

Sample	EDAX analysis[a] (% wt)			Average S[b] (% wt)
	C	O	S	S
ACF10-raw	97.60	2.38	0.20	0.2
ACF10-80 C	96.44	2.42	1.14	6.7
ACF10-150 C	62.97	2.52	34.50	26.3
ACF25-raw	95.41	4.38	0.20	0.2
ACF25-150 C-2 h	94.95	4.03	1.02	4.1
ACF25-150 C-6 h	89.67	2.97	7.36	10.2
ACF25-150 C-24 h	61.14	4.45	34.41	30.5

[a]SEM-EDAX operation conditions: magnification, 100; voltage, 15 kV; scan time, 60 s.

[b]Calculated from QMS analysis.

deposited sulfur can be calculated assuming that the predominant form of elemental sulfur deposited in the ACF pores is S_λ with a density of 1.96 g/cm^3 because of low temperatures used in this study (Berkowitz 1965). Table 3 compares the loss in pore volume to the volume of impregnated sulfur. Column six of this table clearly suggests that the total pore volume lost during the impregnation process was not completely filled with sulfur. Pore blocking must account for a significant fraction of the lost pore volume. The lower temperature resulted in a higher ratio of pore filling. This further supports the hypothesis that pore filling is the dominant mechanism for sulfur deposition at low temperature. At 150°C, all samples showed that less than 50% of the lost pore volume was filled with sulfur. This indicates that most of the pores were blocked, rather than filled. Comparing the volume of sulfur added through impregnation with the loss in volume of medium and big micropores shows that some sulfur must be added into small micropores (SEM-EDAX showed that the excess sulfur was not on the outer surface, Table 2) because it is not possible to have over 100% filling of the pores for ACF10-80C and ACF10-150C. This result suggests that impregnated sulfur cannot be entirely in the form of S_8 because of size restriction (see text below) for the entrance of these large molecules into small micropores. It is more likely that H_2S and O_2, which are much smaller molecules, first entered into small micropores and were then oxidized in situ.

According to Meyer (1964), the sulfur at 150°C should be predominantly in the S_λ form, which is a ring of eight sulfur atoms. Assuming that S_λ is a spherical sulfur allotrope, its diameter is calculated to be 0.73 nm based on the sulfur density. Hsi et al. (2002) also reported a diameter of 0.76 to 0.84 nm depending whether the molecule exists as a ring or as a chain. Fig. 4 shows that ACF25-150C-2 h and ACF25-150C-6 h actually developed more small micropores with diameter below 0.75 nm. This is most probably because the sulfur molecules plugged small micropores with diameter larger than that of one S molecule but smaller than that of two.

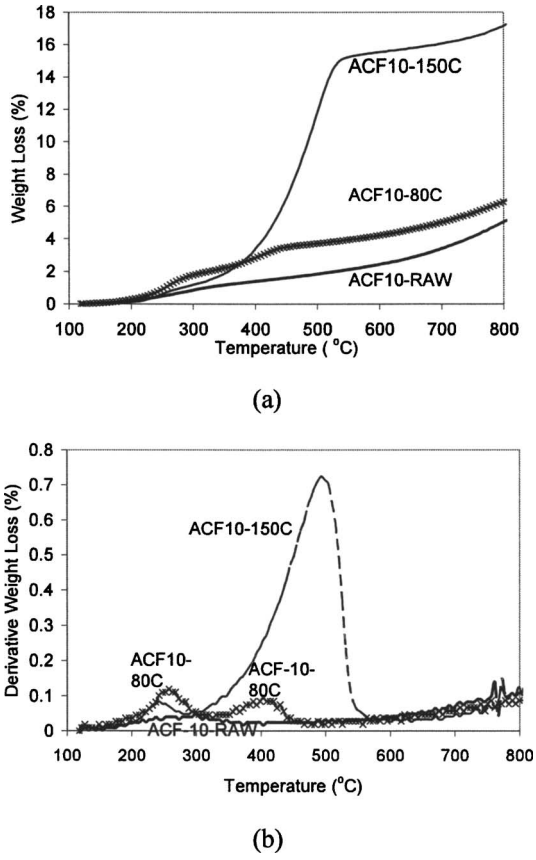

Fig. 5. TGA analysis of ACF-10 before and after sulfur impregnation: (a) Weight loss and (b) derivative weight loss

Stability of Sulfur

Stability of sulfur on the carbon surface is important for practical application since the temperature of mercury laden gas streams is usually above 100°C. Fig. 5 shows TGA analysis of ACF10 before and after sulfur impregnation at 80 and 150°C (it can be assumed that ACF20 and ACF25 impregnated at 150°C would exhibit similar behavior). After heating to 800°C, the raw ACF10 lost less than 2% of its weight, while ACF10-80C and ACF10-150C showed weight loss of 6 and 17%, respectively. These data show that not all the sulfur impregnated on the ACF surface is removed by heating to 800°C in an inert environment (elemental sulfur has a melting point around 119°C and a boiling point about

Table 3. Comparison of Loss in Pore Volume and Volume of Impregnated Sulfur

Sample	Average S (% wt)	S added (mg/g raw ACF)	Volume of S added (cm^3)	V_t loss (cm^3)	Lost V_t filled (%)	Lost V_b+V_m (cm^3)	Lost V_m+V_b filled (%)
ACF10-80 C	6.7	71.8	0.037	0.05	73	0.003	1078
ACF10-150 C	26.3	356.9	0.182	0.36	50	0.143	127
ACF25-150 C-2 h	4.1	42.8	0.022	0.11	20	0.067	33
ACF25-150 C-6 h	10.2	113.6	0.058	0.15	39	0.062	93
ACF25-150 C-24 h	30.5	438.8	0.224	0.83	27	0.452	50

Note: V_b=big micropore volume; V_m=medium micropore volume; and V_t=total pore volume. We assume all sulfur in S_8 form with a density of 1.96 g/cm^3.

444°C). Such behavior is reasonable because some of the sulfur may be embedded into the carbon structure to form C–S complexes. Puri (1970) reported that C–S complexes formed by the reactions between various sulfur containing gases, including S, H_2S, SO_2, and CS_2, and activated carbon are very stable and that heating the complex up to 600°C could not remove all the sulfur impregnated on the carbon surface. Although it is not directly proven in this study, it can be expected that the sulfur vapor created during thermal gravimetric analysis can react with the carbon surface to form these strong bonds at higher temperatures.

The derivative weight loss curve [Fig. 5(b)] shows that there are two weight-loss peaks that appear between 200 and 300 and between 400 and 500°C. The two peaks may represent different bond strengths between the deposited sulfur and carbon structure of the fiber. Fig. 5 also shows that the increase in sulfur impregnation temperature results in greater area for the second peak. Such behavior is expected because higher temperature provides greater energy for creating stronger bonds. Another observation from Fig. 5 is that the elemental sulfur loss occurring at a temperature that is much higher than any of the temperatures used during the impregnation process. Such behavior can be explained by the strength of the interaction between carbon and sulfur and by the porous structure of the sorbent that helps to retain deposited sulfur. Such behavior is beneficial for the mercury removal process as the adsorbed mercury will not be easily released from the sorbent surface if this result can be extrapolated to realistic mercury removal conditions.

Using a method described before (Flynn and Wall 1966), the activation energy can be estimated based on the results shown in Fig. 6. Fig. 6(a) shows the weight loss of ACF10-150C-24 hrs at different heating rates. From the slope of the line correlating $-\log B$ versus $1/T$, it was estimated that the activation energy of the decomposition of the impregnated sulfur on ACF10-150C-24 hr is 90.0 kJ/mol. Compared to a typical C–S chemical bond energy of about 272 kJ/mol (Sanderson 1976), this low activation energy indicates that the sulfur lost during TGA analysis did not form chemical bonds with the carbon surface but is likely bound to the sulfur that remained on the ACF surface at the end of the TGA experiment.

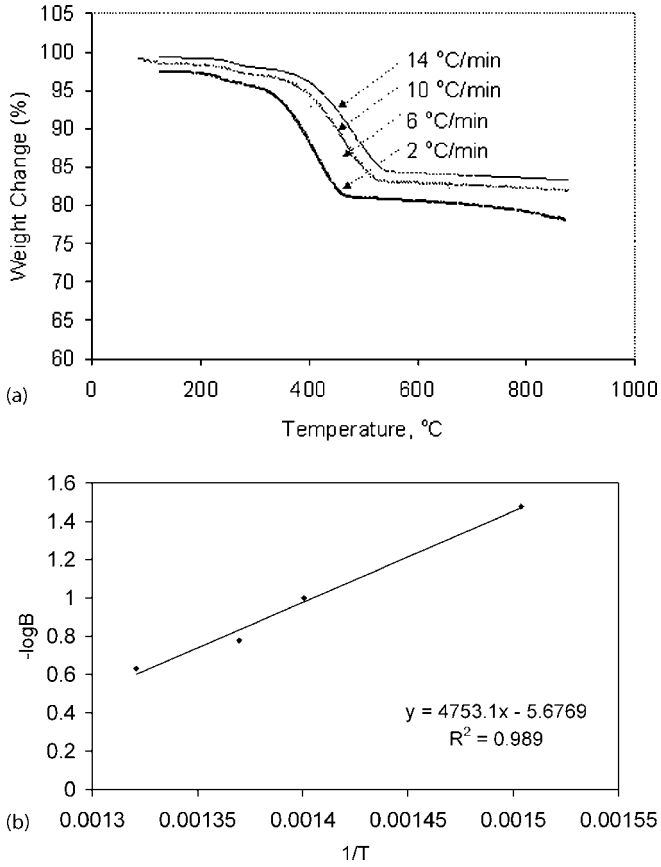

Fig. 6. Estimation of the activation energy for desorption of impregnated sulfur on ACF10-150C-24 hrs: (a) Weight loss at different heating rates and (b) plot of $-\log B$ versus $1/T$

Forms of Sulfur

In order to obtain information on the forms of sulfur on the carbon surface, the QMS 300 was coupled with the TGA 7 to simultaneously monitor the sulfur loss and species released from the ACFs. For this study, a slow nitrogen flow of 12 mL/min and a much higher heating rate of 60°C/min were employed.

Gases exiting the TGA were analyzed by the QMS 300 and the following atomic mass units were monitored: 16 (O), 18 (H_2O), 28 (CO/N_2), 32 (O_2/S), 34 (H_2S), 44 (CO_2), 48 (SO), 64 (SO_2/S_2), 96 (S_3), and 128 (S_4). It was found that major species emitted from ACF10-raw and ACF10-150C were O_2, CO_2, and SO_2. Also, condensed elemental sulfur was clearly observed in the tube at the exit of the TGA furnace and no peaks associated with elemental sulfur were detected by the QMS because of the condensation.

During the TPD (TGA-QMS) analysis, oxygen (possibly from the carbon surface) was released from the carbon surface. For ACF10-raw, only CO_2 was observed, while for ACF10-150C, both SO_2 and CO_2 were released (Fig. 7). These results cannot confirm whether the released sulfur was originally retained on the carbon surface as SO_2 or in some other form. Therefore, these results were combined with XPS study to determine the origin of the SO_2 during heating.

The characteristic XPS spectra for ACF-25 before and after sulfur impregnation are shown in Fig. 8(a). Based on the standard library spectra, the following binding energy data are relevant for this experimental system: around 164.05 eV for free elemental sulfur, 161.8–162.6 eV for chemisorbed sulfur, and higher than 167 eV for oxidized sulfur. Unbound organic sulfur species,

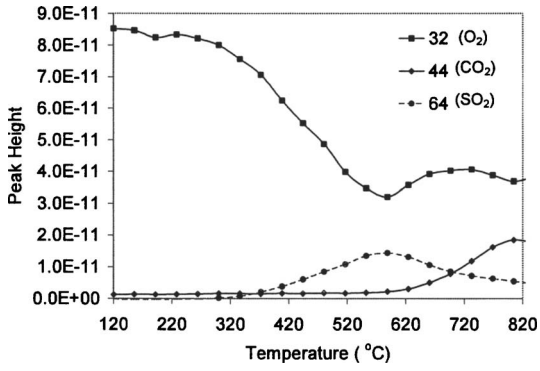

Fig. 7. TPD of ACF10-150C

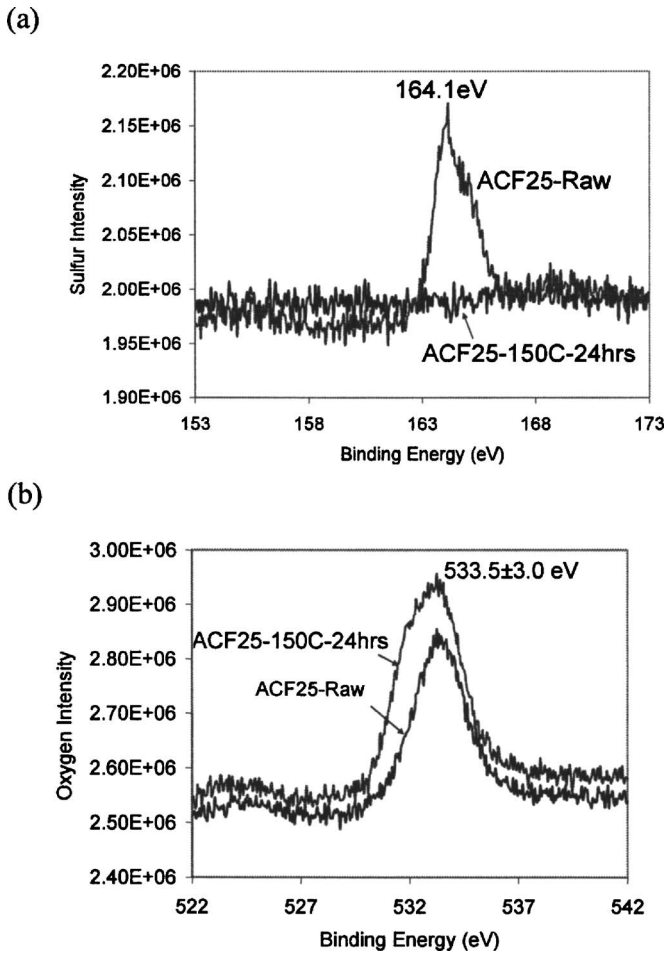

Fig. 8. XPS spectrum of ACF25 before and after sulfur impregnation: (a) Sulfur intensity and (b) oxygen intensity

like thiophene, also show peaks around 164 eV. However, in the presence of oxygen, the generation of these organic species is highly questionable. Fig. 8(a) shows that sulfur on ACF surface is present mainly in free elemental form with negligible amounts of oxidized sulfur forms. Fig. 8(b) shows that the oxygen intensity on ACF surface increased, but not as significant as that of sulfur.

Combining all the observations discussed above, it can be concluded that impregnated sulfur on the carbon surface is mainly present in elemental form. Upon heating the impregnated sorbent, chemisorbed oxygen was released through decomposition of surface functionalities and combined with sulfur to form SO_2 that was observed in the effluent gas during TPD.

It is important to note that contrary to other studies, which found that the major products created during H_2S oxidation on activated carbon surface were both elemental and oxidized sulfur (i.e., sulfuric acid) (Bandosz 1999, 2002; Yan et al. 2004), this study was conducted under dry conditions. Furthermore, the samples used in this study were exposed to relatively high temperatures, which prevented significant retention of water vapor on the carbon surface.

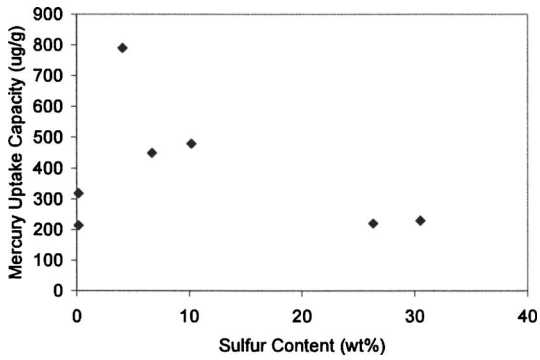

Fig. 9. Correlation of sulfur content with Hg uptake capacity

Impact of Sulfur Content on Mercury Adsorption

Mercury uptake capacity of all adsorbents used in this study as a function of sulfur content is depicted on Fig. 9. It is clear that higher sulfur content does not necessarily lead to greater mercury uptake. Fig. 9 and Table 1 suggest that the sulfur content of around 4% deposited at 150°C produced a sorbent with the highest mercury capacity. Further increase in sulfur content hinders mercury uptake because the excess sulfur blocks or fills the pores of the sorbent, which are required for mercury adsorption. Similar behavior was observed before (Sinha and Walker 1972; Kwon and Vidic 2000). The sulfur utilization ratio was defined as the ratio of the molar amount of sulfur combined with mercury to the total molar amount of impregnated sulfur. The sulfur utilization ratios were calculated and included into Table 1. The low utilization ratios show that most of the sulfur did not react with mercury. Sulfur utilization ratio decreased with a decrease in pore volume, which is likely due reduced accessibility for the reaction with mercury.

Realizing that both sulfur content and pore structure of the sorbent are important, it is likely that the sorbent impregnated with a sulfur monolayer would offer best performance for mercury uptake. It is reasonable to suggest that sulfur which deposits on the sorbent surface in the second layer would block the access to the first layer and, at the same time, reduce the pore volume of the sorbent.

Table 4. Effect of Pore Volume of Raw ACFs on Hg Uptake Capacity

Sample name	V_s (cm^3/g)	V_m (cm^3/g)	V_b (cm^3/g)	V_s+V_m (cm^3/g)	V_m+V_b (cm^3/g)	Total (cm^3/g)	Hg uptake capacity ($\mu g/g$)
ACF-10-raw	0.274	0.039	0.065	0.313	0.104	0.378	214
ACF-20-raw	0.258	0.104	0.329	0.362	0.433	0.691	271
ACF-25-raw	0.263	0.101	0.489	0.364	0.59	0.853	319
Slope b	−4544	246.7	244.5	1646	209.5	215.8	
Coefficient R^2	0.501	0.757	0.992	0.819	0.977	0.983	

Table 5. Effect of Surface Area of Raw ACFs on Hg Uptake Capacity

Sample name	S_s (m^2/g)	S_m (m^2/g)	S_b (m^2/g)	S_s+S_m (m^2/g)	S_m+S_b (m^2/g)	Total (m^2/g)	Hg uptake capacity ($\mu g/g$)
ACF-10-raw	485	528	196	1012	724	920	214
ACF-20-raw	578	388	762	966	1150	1453	271
ACF-25-raw	398	533	973	931	1506	1950	319
Slope b	−2.65	−0.01	0.128	−1.29	0.13	0.10	
Coefficient R^2	0.215	0.003	0.957	0.999	1	0.999	

Impact of Pore Volume and Surface Area on Mercury Adsorption

The effects of pore volume and surface area were analyzed separately for raw ACFs and for ACF25 impregnated with sulfur. The pores were divided into three groups as described earlier: small, medium, and big micropores. The pore volume and surface area of each group were determined from surface area analysis. These values were correlated with observed mercury uptake using linear regression and the slope of the linear fit to experimental data (the value of the coefficient b in the expression $q_{Hg}=a+bx$) indicates the significance of a given parameter for Hg uptake. Sulfur impregnated ACFs were analyzed separately from virgin ACFs due to the important contribution of impregnated sulfur on mercury uptake. These analyses were done in an attempt to find the most important pore size region for Hg uptake by virgin and impregnated ACFs.

Table 4 shows the effect of pore volume on Hg uptake capacity of the raw ACFs. V_b, V_s+V_m, V_m+V_b, and the total pore volume all showed good correlation with Hg uptake. Although V_s+V_m has the highest b value, its R^2 is much smaller than that of the others. It appears that medium and big micropores contribute the most to Hg uptake. Because small micropores do not represent a major contribution to mercury uptake by virgin ACFs, it can be concluded that mercury adsorption on virgin ACFs at 140°C is not achieved through physisorption (Dubinin 1960). This finding supports previous suggestion that mercury uptake by carbonaceous sorbents at 140°C is mainly due to chemisorption (Kwon et al. 2002). As shown in Table 5, attempts to correlate fractions of surface area associated with small, medium, and big micropores with mercury uptake support the conclusions discussed above because the surface area of medium and big micropores (S_m+S_b) provided the best correlation with Hg uptake.

In addition to the impacts of surface morphology that were investigated in this study, it is important to consider the impact of surface chemistry on mercury uptake (Krishnan et al. 1994; Li et al. 2003). Attempts to correlate the pore volume and surface area of sulfur impregnated ACF25 and mercury uptake resulted in fairly small R^2 values, which suggests that factors other than surface morphology affect Hg uptake. This conclusion is expected because HgS formation is believed to be the dominant mechanism for mercury uptake by sulfur impregnated sorbents.

Conclusions

Previous studies showed that not only the sulfur content, but the forms and distribution of sulfur on the adsorbent surface, also play an important role in mercury uptake. Under the experimental conditions used in this study, the following conclusions were obtained.

Sulfur was impregnated mainly as elemental sulfur and the amount of sulfur deposited on the ACF increased with an increase in impregnation temperature; higher temperature leads to more uniform sulfur distribution inside the sorbent pores.

More sulfur was found in the internal pores than on the external surface layer; the impregnation process can be explained by a combination of pore filling and monolayer adsorption, with the former mechanism predominating at low temperatures.

Although SO_2 was observed in the TPD effluent gas stream, sulfur was mainly impregnated as elemental sulfur, with negligible amount in the oxidized form.

In the absence of sulfur, the mercury adsorption capacity can be correlated with surface area and pore volume with medium ($0.72<d<0.90$ nm) and big micropores ($d>0.90$ nm) being more important for mercury uptake.

Acknowledgments

Funding for this work was provided by the National Science Foundation (BES-0202015). The writers would like to thank Dr. Waldeck's group at the Department of Chemistry, University of Pittsburgh for providing assistance with XPS analysis. The writers are also grateful to Dr. Joseph Hayes at American Kynol, Inc. for providing ACF samples and for useful discussions.

References

Aranovich, G. L., and Donohue, M. D. (1995). "Adsorption-isotherms for microporous adsorbents." *Carbon*, 33(10), 1369–1375.

Bagreev, A., Adib, F., and Bandosz, T. J. (1999). "Initial heats of H_2S adsorption on activated carbons: Effect of surface features." *J. Colloid Interface Sci.*, 219(2), 327–332.

Bagreev, A., and Bandosz, T. J. (2001). "H_2S adsorption/oxidation on unmodified activated carbons: importance of prehumidification." *Carbon*, 39(15), 2303–2311.

Bagreev, A., and Bandosz, T. J. (2002). "A role of sodium hydroxide in the process of hydrogen sulfide adsorption/oxidation on caustic-impregnated activated carbons." *Ind. Eng. Chem. Res.*, 41(4), 672–679.

Bagreev, A., Rahman, H., and Bandosz, T. J. (2001). "Thermal regeneration of a spent activated carbon previously used as hydrogen sulfide adsorbent." *Carbon*, 39(9), 1319–1326.

Bandosz, T. J. (1999). "Effect of pore structure and surface chemistry of virgin activated carbons on removal of hydrogen sulfide." *Carbon*, 37(3), 483–491.

Bandosz, T. J. (2002). "On the adsorption/oxidation of hydrogen sulfide on activated carbons at ambient temperatures." *J. Colloid Interface Sci.*, 246(1), 1–20.

Berkowitz, J. (1965). "Molecular composition of sulfur vapor." *Elemental sulfur*, B. Meyer, ed., Interscience, New York, 125–160.

Boki, K., and Tanada, S. (1980). "Adsorption of hydrogen sulfide on activated carbon." *Chem. Pharm. Bull. (Tokyo)*, 28(4), 1270–1275.
Chang, R., and Offen, G. (1995). "Mercury emission control technologies: An EPRI synopsis." *Power Eng. J.*, 99(11), 51–57.
Daza, L., Mendioroz, S., and Pajares, J. A. (1989). "Influence of texture and chemical composition on sulphur deposition onto sepiolites." *Appl. Clay Sci.*, 4(5-6), 389–402.
Daza, L., Mendioroz, S., and Pajares, J. A. (1993). "Mercury elimination from gaseous streams." *Appl. Catal., B*, 2, 277–287.
Dubinin, M. M. (1960). "The potential theory of adsorption of gases and vapors for adsorbents with energetically nonuniform surfaces." *Chem. Rev. (Washington, D.C.)*, 60(2), 235–241.
EPA. (1997). *Mercury study Rep. to Congress*, Vol. II, Washington, D.C.
Flora, J. R. V., Hargis, R. A., O'Dowd, W. J., Pennline, H. W., and Vidic, R. D. (2003). "Modeling sorbent injection for mercury control in baghouse filters: II—Pilot-scale studies and model evaluation." *J. Air Waste Manage. Assoc.*, 53(4), 489–496.
Flynn, J. H., and Wall, L. A. (1966). "A quick, direct method for the determination of activation energy from thermogravimetric data." *Polym. Lett.*, 4, 323–328.
Guijarro, M. I., Mendioroz, S., and Munoz, V. (1998). "Effect of morphology of sulfurized materials in the retention of mercury from gas streams." *Ind. Eng. Chem. Res.*, 37(3), 1088–1094.
Hsi, H. C., Rood, M. J., Rostam-Abadi, M., Chen, S. G., and Chang, R. (2001). "Effects of sulfur impregnation temperature on the properties and mercury adsorption capacities of activated carbon fibers (ACFs)." *Environ. Sci. Technol.*, 35(13), 2785–2791.
Hsi, H. C., Rood, M. J., Rostam-Abadi, M., Chen, S. G., and Chang, R. (2002). "Mercury adsorption properties of sulfur-impregnated adsorbents." *J. Environ. Eng.*, 128(11), 1080–1089.
Korpiel, J. A., and Vidic, R. D. (1997). "Effect of sulfur impregnation method on activated carbon uptake of gas-phase mercury." *Environ. Sci. Technol.*, 31(8), 2319–2325.
Krishnan, S. V., Gullett, B. K., and Jozewicz, W. (1994). "Sorption of elemental mercury by activated carbons." *Envir. Toxicol. Chem.*, 28(8), 1506–1512.
Kwon, S., Borguet, E., and Vidic, R. D. (2002). "Impact of surface heterogeneity on mercury uptake by carbonaceous sorbents under UHV and atmospheric pressure." *Environ. Sci. Technol.*, 36(19), 4162–4169.
Kwon, S., and Vidic, R. D. (2000). "Evaluation of two sulfur impregnation methods on activated carbon and bentonite for the production of elemental mercury sorbents." *Environ. Eng. Sci.*, 17(6), 303–313.
Lee, W. H., and Reucroft, P. J. (1999). "Vapor adsorption on coal- and wood-based chemically activated carbons—(III)—NH_3 and H_2S adsorption in the low relative pressure range." *Carbon*, 37(1), 21–26.
Li, Y. H., Lee, C. W., and Gullett, B. K. (2003). "Importance of activated carbon's oxygen surface functional groups on elemental mercury adsorption." *Fuel*, 82(4), 451–457.
Liu, W., Vidic, R. D., and Brown, T. D. (1998). "Optimization of sulfur impregnation protocol for fixed bed application of activated carbon-based sorbents for gas-phase mercury removal." *Environ. Sci. Technol.*, 32(4), 531–538.
Meyer, B. (1964). "Solid allotropes of sulphur." *Chem. Rev.*, 64, 429–451.
Otani, Y., Emi, H., Kanaoka, C., Uchiwa, I., and Nishino, H., (1988). "Removal of mercury vapor from air with sulfur-impregnated adsorbents." *Environ. Sci. Technol.*, 22, 708–711.
Puri, B. R. (1970). *Surface complexes on carbon*, Dekker, New York.
Sanderson, R. T. (1976). *Chemical bonds and bond energy*, Academic, New York.
Sinha, R. K., and Walker, P. L. (1972). "Removal of mercury by sulfurized carbons." *Carbon*, 10, 754–756.
Yan, R., Chin, T., Ng, Y. L., Duan, H., Liang, D. T., and Tay, J. H. (2004). "Influence of surface properties on the mechanism of H_2S removal by alkaline activated carbons." *Environ. Sci. Technol.*, 38(1), 316–323.
Yan, R., Liang, D. T., Tsen, L., and Tay, J. H. (2002). "Kinetics and mechanisms of H_2S adsorption by alkaline activated carbon." *Environ. Sci. Technol.*, 36(20), 4460–4466.